Preprints of the 21st IFAC World Congress (Virtual)
Berlin, Germany, July 12-17, 2020

Motion planning for a class of boundary controlled 1D port-Hamiltonian systems ⋆

Bastian Biedermann Thomas Meurer

Chair of Automatic Control, Faculty of Engineering, Kiel University, Kiel, Germany (e-mail: {basb,tm}@tf.uni-kiel.de).

Abstract: A flatness-based approach for motion planning for a class of boundary controlled port-Hamiltonian systems with distributed parameters is presented. The goal is to achieve open-loop output tracking or finite-time transitions between steady states or operating profiles. Introducing new (fictious) boundary conditions in terms of so-called flat outputs, the port-Hamiltonian system is reformulated as a Cauchy problem in the spatial domain. The parametrization of any system variable and input by the flat output is computed using two different solution approaches. By assigning a suitable desired trajectory for the flat output, the input parametrization yields the feedforward control law to solve the motion planning task. The presented theory is applied to the wave equation with spatially varying parameters and is evaluated by numerical calculations and simulations.

Keywords: Motion Planning, Port-Hamiltonian System, Boundary Control, Trajectory Planning, Distributed Parameter System, Partial Differential Equation, Wave Equation

1. INTRODUCTION

The design and realization of a feedforward control to achieve finite-time transitions between operating points or open-loop output tracking is an important task in control applications, see, e.g., Meurer (2012) and the references therein. This motion planning problem is complicated when dealing with partial differential equations and even further if spatially and time varying system parameters arise in the mathematical process models.

For finite-dimensional linear and nonlinear systems the property of differential flatness (Fliess et al., 1995; Rothfuss et al., 1996) has enabled the development of efficient techniques to solve the motion planning and the tracking control problem (Rothfuß, 1997; Fliess et al., 1999). Flatness refers to the existence of a so-called flat or basic output that allows to (differentially) parametrize the system states and inputs. As a consequence, by assigning a suitably regular desired trajectory for the flat output the evaluation of the input parametrization yields the feedforward control that under nominal conditions realizes the state trajectory obtained by substituting the desired flat output trajectory into the state parametrization. This equivalence property has been successfully exploited to solve motion planning problems for distributed parameter systems governed by partial differential equations.

The application of flatness-based trajectory planning for partial differential equations is well studied given a single spatial coordinate (Laroche et al., 2000; Petit and Rouchon, 2002; Lynch and Rudolph, 2002; Dunbar et al., 2003; Meurer and Zeitz, 2005; Rudolph and Woittennek, 2008; Woittennek, 2011; Meurer, 2012). In addition, extensions to systems with higher dimensional spatial domain are available as presented, e.g., by Meurer (2012); Meurer and Kugi (2009); Meurer (2011). Given parabolic partial differential equations the states and inputs are parametrized using formal power series or fractional differentiation operators. In addition an approach using formal integration is proposed by Schörkhuber et al. (2013) that allows a systematic extension of the flatness-based motion planning concept to general semilinear parabolic partial differential equations with boundary actuation. To assess convergence the flat output is typically restricted to certain Gevrey class functions, whose derivatives can be suitably bounded. To address input and state constraints recently an optimization approach was proposed by Andrej and Meurer (2018), where the trajectory planning for the flat output is addressed using an integrator chain. For systems evolving wave dynamics delayed and advanced arguments emerge in the state and input parametrizations that reflect the finite speed of wave propagation (Petit and Rouchon, 2002).

In the present contribution flatness-based motion planning is applied to infinite-dimensional port-Hamiltonian systems. This class of systems covers many physical processes arising in thermodynamics, mechanics, electrodynamics or mechatronics as shown by van der Schaft (2006); Duindam et al. (2009). Favorably their stability properties can be assessed systematically in terms of their system operator and the input output pairing providing an immediate connection to passive systems and stability in the sense of Lyapunov. Boundary controlled distributed parameter port-Hamiltonian systems without internal energy dissipation describe various partial differential equations including the wave equation, the Timoshenko beam or certain biharmonic equations (Le Gorrec et al., 2005; Jacob and Zwart, 2012). Subsequently, motion planning is analyzed for a class of boundary controlled port-Hamiltonian systems.

⋆ The work was supported by Deutsche Forschungsgemeinschaft (DFG)/Agence Nationale de la Recherche (ANR) project INFIDHEM, ID ANR-16-CE92-0028.

This paper is organized as follows. In Sec. 2 the considered class of port-Hamiltonian systems and the motion planning problem are introduced. The main results are provided in Sec. 3. First, the port-Hamiltonian system is rearranged into a Cauchy problem. Secondly, two solution approaches to explicitly determine the parametrization are presented. The applications of the proposed methods to the wave equation is presented in Sec. 4, providing also numerical results that underline the performance of these approaches. Some final remarks in Sec. 5 conclude the paper.

2. PROBLEM FORMULATION

In the following the motion planning problem for distributed parameter port-Hamiltonian systems is investigated. The investigated class of boundary controlled first order port-Hamiltonian systems as presented by Le Gorrec et al. (2005); Jacob and Zwart (2012) is considered as

$$\partial_t \boldsymbol{x}(z,t) = \mathcal{J}\boldsymbol{x}(z,t), \quad t>0, \tag{1a}$$
$$\boldsymbol{x}(z,0) = \boldsymbol{x}_0(z) \in \mathcal{D}(\mathcal{J}), \tag{1b}$$
$$\boldsymbol{0} = W\mathcal{H}(a)\boldsymbol{x}(a,t), \tag{1c}$$
$$\boldsymbol{u}(t) = B\mathcal{H}(b)\boldsymbol{x}(b,t) \tag{1d}$$

on the spatial interval $z \in [a,b] \subseteq \mathbb{R}$ with $a < b$. The matrices for the boundary conditions are $B \in \mathbb{R}^{m\times n}$ and $W \in \mathbb{R}^{(n-m)\times n}$. The matrix $\mathcal{H} \in L^\infty([a,b];\mathbb{R}^{n\times n})$ is positive definite, i.e., there exist $\alpha,\beta \in \mathbb{R}^+$ such that $\alpha I \preceq \mathcal{H}(z) \preceq \beta I$. Moreover, $P_0 = -P_0^\mathsf{T} \in \mathbb{R}^{n\times n}$ and $P_1 = P_1^\mathsf{T} \in \mathbb{R}^{n\times n}$ is invertible. The state space is given by $\mathcal{X} = L^2([a,b];\mathbb{R}^n)$ with the inner product

$$\langle \boldsymbol{f},\boldsymbol{g}\rangle_{\mathcal{X}} = \frac{1}{2}\int_a^b \boldsymbol{f}^\mathsf{T}(z)\mathcal{H}(z)\boldsymbol{g}(z)\,\mathrm{d}z. \tag{2}$$

In order to verify that the operator

$$\mathcal{J}\boldsymbol{x}(z,t) = P_1\partial_z\left(\mathcal{H}(z)\boldsymbol{x}(z,t)\right) + P_0\mathcal{H}(z)\boldsymbol{x}(z,t) \tag{3}$$

generates a C_0-semigroup, the boundary flows $\boldsymbol{f} \in \mathcal{X}$ and boundary efforts $\boldsymbol{e} \in \mathcal{X}$, i.e.,

$$\begin{bmatrix}\boldsymbol{f}\\ \boldsymbol{e}\end{bmatrix} = \frac{1}{\sqrt{2}}\begin{bmatrix}P_1 & -P_1\\ I & I\end{bmatrix}\begin{bmatrix}\mathcal{H}(a)\boldsymbol{x}(a,t)\\ \mathcal{H}(b)\boldsymbol{x}(b,t)\end{bmatrix} = R_0\begin{bmatrix}\mathcal{H}(a)\boldsymbol{x}(a,t)\\ \mathcal{H}(b)\boldsymbol{x}(b,t)\end{bmatrix}$$

with $R_0 \in \mathbb{R}^{2n\times 2n}$ are investigated. Thus, the boundary conditions of (1) can be expressed as

$$\begin{bmatrix}\boldsymbol{u}(t)\\ \boldsymbol{0}\end{bmatrix} = \begin{bmatrix}0 & B\\ W & 0\end{bmatrix}\begin{bmatrix}\mathcal{H}(a)\boldsymbol{x}(a,t)\\ \mathcal{H}(b)\boldsymbol{x}(b,t)\end{bmatrix} = W_B\begin{bmatrix}\boldsymbol{f}\\ \boldsymbol{e}\end{bmatrix}$$

with the matrix

$$W_B = \begin{bmatrix}0 & B\\ W & 0\end{bmatrix}R_0^{-1} = \frac{1}{\sqrt{2}}\begin{bmatrix}-BP_1^{-1} & B\\ WP_1^{-1} & W\end{bmatrix} \in \mathbb{R}^{n\times 2n}. \tag{4}$$

In reference to (Jacob and Zwart, 2012, Remark 11.3.3), the operator $\mathcal{J}$ defined in (3) with domain

$$\mathcal{D}(\mathcal{J}) = \left\{\boldsymbol{x}\in\mathcal{X} \mid \mathcal{H}\boldsymbol{x} \in H^1\left([a,b];\mathbb{R}^n\right), \begin{bmatrix}\boldsymbol{f}\\ \boldsymbol{e}\end{bmatrix} \in \ker W_B\right\}$$

is an infinitesimal generator of a C_0-semigroup if

$$\operatorname{rank}(W_B) = n, \tag{5a}$$
$$W_B\begin{bmatrix}0 & I\\ I & 0\end{bmatrix}W_B^\mathsf{T} \succeq 0. \tag{5b}$$

Conditions (5) are assumed to hold true subsequently.

Steady states denoted by the pair $(\boldsymbol{x}_\mathrm{s}(z),\boldsymbol{u}_\mathrm{s})$ are defined by the elliptic equations

$$\boldsymbol{0} = \mathcal{J}\boldsymbol{x}_\mathrm{s}(z), \quad \boldsymbol{0} = W\mathcal{H}(a)\boldsymbol{x}_\mathrm{s}(a), \quad \boldsymbol{u}_\mathrm{s} = B\mathcal{H}(b)\boldsymbol{x}_\mathrm{s}(b). \tag{6}$$

The main objective of this contribution is to determine the feedforward input trajectory $\boldsymbol{u}(t)$ to achieve the transition from an initial steady state $(\boldsymbol{x}_{0,\mathrm{s}}(z),\boldsymbol{u}_{0,\mathrm{s}})$ to a desired final steady state $(\boldsymbol{x}_{\tau,\mathrm{s}}(z),\boldsymbol{u}_{\tau,\mathrm{s}})$ along a predefined spatial-temporal transition path within $t\in[0,\tau]$. Assuming that the initial state is a steady state of (1), without loss of generality consider $\boldsymbol{x}_0(z) = \boldsymbol{0}$.

3. FLATNESS–BASED MOTION PLANNING

Motion planning refers to the determination of the input trajectory to achieve a desired trajectory for the system output or state, respectively. To achieve this, a flatness based approach is considered by constructing a flat output parametrizing the state and input.

3.1 Cauchy problem formulation

Subsequently, the port-Hamiltonian system (1) is expressed as a Cauchy problem in the spatial coordinate. The solution by a Cauchy boundary value problem for hyperbolic distributed parameter systems with constant coefficients is investigated by Woittennek (2011). However, this work investigates another problem formulation. First, the used state variables are the energy variables due to the port-Hamiltonian system. Secondly, spatial variable coefficients are considered. The system dynamics (1a) in terms of the operator (3) are expanded, i.e.,

$$\begin{aligned}\partial_t\boldsymbol{x}(z,t) = &\left(P_1\partial_z\mathcal{H}(z) + P_0\mathcal{H}(z)\right)\boldsymbol{x}(z,t) + \\ &P_1\mathcal{H}(z)\partial_z\boldsymbol{x}(z,t).\end{aligned} \tag{7}$$

Rearranging (7) with respect to the spatial derivative yields

$$\begin{aligned}P_1\mathcal{H}(z)\partial_z\boldsymbol{x}(z,t) = &\partial_t\boldsymbol{x}(z,t) - \\ &\left(P_1\partial_z\mathcal{H}(z) + P_0\mathcal{H}(z)\right)\boldsymbol{x}(z,t).\end{aligned} \tag{8}$$

Recalling that P_1 and $\mathcal{H}(z)$ are invertible by definition, (8) can be reformulated as

$$\partial_z\boldsymbol{x}(z,t) = \Gamma_1(z)\partial_t\boldsymbol{x}(z,t) - \Gamma_0(z)\boldsymbol{x}(z,t). \tag{9}$$

The matrices $\Gamma_1(z)$ and $\Gamma_0(z)$ are given by

$$\Gamma_1(z) = \mathcal{H}^{-1}(z)P_1^{-1}, \tag{10a}$$
$$\Gamma_0(z) = \mathcal{H}^{-1}(z)\partial_z\mathcal{H}(z) + \mathcal{H}^{-1}(z)P_1^{-1}P_0\mathcal{H}(z). \tag{10b}$$

To introduce a flat output consider

$$\boldsymbol{y}(t) = C\mathcal{H}(a)\boldsymbol{x}(a,t), \tag{11}$$

which imposes a new boundary conditions for (1) so that

$$\begin{bmatrix}W\\ C\end{bmatrix}\mathcal{H}(a)\boldsymbol{x}(a,t) = \begin{bmatrix}\boldsymbol{0}\\ \boldsymbol{y}(t)\end{bmatrix}. \tag{12}$$

In principle this corresponds to interchanging the input and flat output. This is possible if there exists a matrix $C\in\mathbb{R}^{m\times n}$ so that

$$\det\left(\begin{bmatrix}W\\ C\end{bmatrix}\right) \neq 0. \tag{13}$$

Note that the matrix (4) reads

$$W_B = \begin{bmatrix}C & 0\\ W & 0\end{bmatrix}R_0^{-1} = \frac{1}{\sqrt{2}}\begin{bmatrix}CP_1^{-1} & B\\ WP_1^{-1} & W\end{bmatrix}$$

in this case, which verifies that (13) denotes one equivalent condition for a well-posed port-Hamiltonian system in

terms of (5a). Thus, the boundary conditions (12) can be expressed as

$$\boldsymbol{x}(a,t) = \mathcal{H}^{-1}(a) \begin{bmatrix} W \\ C \end{bmatrix}^{-1} \begin{bmatrix} \mathbf{0} \\ \boldsymbol{y}(t) \end{bmatrix} = M\boldsymbol{y}(t) \tag{14}$$

with $M \in \mathbb{R}^{n\times m}$. Since $\mathcal{J}$ is the infinitesimal generator of a C_0-semigroup, the Laplace transformation of (9), (10) exists and is given by

$$\partial_z \hat{\boldsymbol{x}}(z,s) = (\Gamma_1(z)s - \Gamma_0(z))\,\hat{\boldsymbol{x}}(z,s), \tag{15}$$

with $\hat{\boldsymbol{x}}(z,s) = \mathcal{L}\{\boldsymbol{x}(z,t)\}$. Combining (15) and the Laplace transformation of (14) yields the Cauchy problem

$$\partial_z \hat{\boldsymbol{x}}(z,s) = \Gamma(z,s)\hat{\boldsymbol{x}}(z,s), \tag{16a}$$
$$\hat{\boldsymbol{x}}(a,s) = M\hat{\boldsymbol{y}}(s) \tag{16b}$$

with respect to the independent coordinate z, where

$$\Gamma(z,s) = \Gamma_1(z)s - \Gamma_0(z). \tag{17}$$

The input (1d) then follows as

$$\hat{\boldsymbol{u}}(s) = B\mathcal{H}(b)\hat{\boldsymbol{x}}(b,s)$$

with $\hat{\boldsymbol{x}}(z,s)$ from (16).

Remark 1. Note that (16) is not explicitely restricted to port-Hamiltonian systems (1) but can also be achieved for more general setups. Nevertheless, the port-Hamiltonian framework offers a proper system structure and required conditions like matrix inversions in reference to (10).

In the following, two solution approaches to achieve an expression for the state and input by a flat output parametrization are presented.

3.2 Formal integration

One solution approach to determine $\hat{\boldsymbol{x}}(z,s)$ from (16) in terms of $\hat{\boldsymbol{y}}(s)$ is to use formal integration over the spatial domain. This yields

$$\hat{\boldsymbol{x}}(z,s) = M\hat{\boldsymbol{y}}(s) + \int_a^z \Gamma(\eta,s)\hat{\boldsymbol{x}}(\eta,s)\,\mathrm{d}\eta, \tag{18}$$

and represents an implicit parametrization of $\hat{\boldsymbol{x}}(z,s)$ in terms of $\hat{\boldsymbol{y}}(s)$. The latter can be rendered explicit by introducing the iteration rule

$$\hat{\boldsymbol{x}}^{[0]}(z,s) = M\hat{\boldsymbol{y}}(s), \tag{19a}$$
$$\hat{\boldsymbol{x}}^{[k]}(z,s) = \hat{\boldsymbol{x}}^{[0]}(z,s) + \int_a^z \Gamma(\eta,s)\hat{\boldsymbol{x}}^{[k-1]}(\eta,s)\,\mathrm{d}\eta \tag{19b}$$

for $k \in \mathbb{N}$. The limit of the iteration can be formally written as

$$\hat{\boldsymbol{x}}^{[\infty]}(z,s) = A(z,s)M\hat{\boldsymbol{y}}(s), \tag{20a}$$
$$A(z,s) = \sum_{k=0}^{\infty} \Lambda^{[k]}(z,s) \tag{20b}$$

with the matrix recursion

$$\Lambda^{[k]}(z,s) = \begin{cases} I, & k = 0, \\ \displaystyle\int_a^z \Gamma(\eta,s)\Lambda^{[k-1]}(\eta,s)\,\mathrm{d}\eta, & k > 0. \end{cases} \tag{21}$$

Herein, I is the identity matrix. This recursion represents the Peano-Baker series in dependency of s, which can be for the evaluation of (20) simply considered as a parameter. The verification of (20), (21) is summarized in the Appendix A.

However, depending on the considered problem and hence the matrices $\Gamma_i(z)$ the computational costs to calculate the series coefficients may be large. Thus, for practical reasons only a finite number of recursions is performed, so that (20b) is replaced by

$$A(z,s) \approx \sum_{k=0}^{K} \Lambda^{[k]}(z,s) \tag{22}$$

for some sufficiently large integer $K \in \mathbb{N}$.

Remark 2. The Peano-Baker series is known to converge assuming continuity or continuous differentiability of the matrices $\Gamma_i(z)$, e.g., as shown in DaCunha (2005). However, this does not ensure the convergence of (20) transformed into the time domain, i.e.,

$$\boldsymbol{x}^{[\infty]}(z,t) = A(z,\partial_t) \circ M\boldsymbol{y}(t), \tag{23}$$

where $A(z,\partial_t)$ has to be interpreted formally as a differentiation operator applied to the flat output. Subsequently, the general convergence analysis of (23) is omitted due to page restrictions but follows in principle the lines of Meurer and Kugi (2009); Schörkhuber et al. (2013).

For the special case of constant matrices the following remark provides a general solution.

Remark 3. If $\Gamma_1(z) = \Gamma_1$ and $\Gamma_0(z) = \Gamma_0$ are constant matrices, i.e., $\mathcal{H}(z) = \mathcal{H}$ has only constant entries, then (17) reduces to $\Gamma(s) = \Gamma_1 s - \Gamma_0$. As a result, (20b) evaluates to

$$A(z,s) = \sum_{k=0}^{\infty} \frac{\Gamma^k(s)}{k!}(z-a)^k = e^{\Gamma(s)(z-a)}, \tag{24}$$

which is the matrix exponential. This in particular implies that the time domain expression can be obtained by determining (24), evaluating the product with the flat output according to (20a) and using the properties of the inverse Laplace transformation.

3.3 Numerical inverse Laplace transformation

In general, the existence of an analytic solution for (20), (21) and the corresponding inverse Laplace transformation is not guaranteed for the case of non-constant coefficients. Although a numerical solution is given by (22), the corresponding computational complexity may be too large because the solution only exists for the series limit, i.e., $K \to \infty$. To solve this problem, an alternative numerical solution approach is presented in the following.

First, a numerical method so solve the Cauchy problem in z needs to be specified, i.e.,

$$\hat{\boldsymbol{x}}(z_i,s) = \boldsymbol{f}\left(z_{i-1}, z_i, \Delta z, \hat{\boldsymbol{x}}(z_{i-1},s)\right), \tag{25a}$$
$$\hat{\boldsymbol{x}}(z_0,s) = M\hat{\boldsymbol{y}}(s) \tag{25b}$$

with $i \in \{1,2,\ldots,N\}$, stepsize $\Delta z = (b-a)/N$, $N \in \mathbb{N}$, $z_0 = a$, $z_N = b$ and $\boldsymbol{f}(z_{i-1}, z_i, \Delta z, \hat{\boldsymbol{x}}(z_{i-1},s))$ describing the used discretization scheme. Note that a single step discretization scheme is described for illustration. A multi step method is also valid. Second, an algorithm for solving the inverse Laplace transformation needs to be specified. Subsequently, the inverse Laplace transformation using concentrated matrix exponential method proposed by Horváth et al. (2020) is used. Given the Laplace transformation $\hat{h}(s)$ of $h(t)$, the method calculates the value of an $h(\tau)$ at time $\tau > 0$ in terms of

$$h(\tau) \approx \frac{1}{\tau} \sum_{k=0}^{K} \eta_k \hat{h}\left(\frac{\beta_k}{\tau}\right), \tag{26}$$

where η_k and β_k are parameters. This procedure offers an improved numerical stability and a more accurate approximation, e.g., compared to the Euler or Gather method (Abate and Whitt, 2006; Horváth et al., 2020). The accuracy depends on the chosen order. In this case a very high order is considered, since the calculation for the feedforward control are done offline. Third, the state $\boldsymbol{x}(z_i, t_j)$ at the spatial coordinate z_i and at time t_j is calculated by combining (25) and (26), i.e.,

$$\boldsymbol{x}(z_i, t_j) \approx \frac{1}{t_j} \sum_{k=0}^{K} \eta_k \hat{\boldsymbol{x}}\left(z_i, \frac{\beta_k}{t_j}\right), \tag{27}$$

where t_j is an element from the set

$$t_j \in \{t_0, \dots, t_T\}, \quad j \in \{0, 1, \dots, T\} \tag{28}$$

with $T \in \mathbb{N}$ and $t_0 > 0$. Finally, the input is calculated by

$$\boldsymbol{u}(t_j) = B\mathcal{H}(b)\boldsymbol{x}(b, t_j) = B\mathcal{H}(b)\boldsymbol{x}(z_N, t_j). \tag{29}$$

4. WAVE EQUATION

In the following, the results of Sec. 3 are used to solve the motion planning problem for the wave equation

$$\begin{aligned} \rho(z)\partial_t^2 w(z,t) &= \partial_z\left(\vartheta(z)\partial_z w(z,t)\right), \quad t > 0, \\ w(z,0) = 0, &\quad \partial_t w(z,0) = 0 \\ \vartheta(0)\partial_z w(0,t) = 0, &\quad \vartheta(3)\partial_z w(3,t) = u(t), \end{aligned} \tag{30}$$

where $w(z,t)$ is the displacement, $\vartheta(z)$ is Young's modulus and $\rho(z)$ is the material density. Introducing the state variables

$$\boldsymbol{x}(z,t) = \begin{bmatrix} \rho(z)\partial_t w(z,t) \\ \partial_z w(z,t) \end{bmatrix}, \tag{31}$$

(30) can be formulated as a port-Hamiltonian system according to (1), i.e.,

$$\begin{aligned} \partial_t \boldsymbol{x}(z,t) &= \begin{bmatrix} 0 & 1 \\ 1 & 0 \end{bmatrix} \partial_z \left(\begin{bmatrix} \frac{1}{\rho(z)} & 0 \\ 0 & \vartheta(z) \end{bmatrix} \boldsymbol{x}(z,t) \right), \quad t > 0, \\ 0 &= [0\ 1]\,\mathcal{H}(0)\boldsymbol{x}(0,t), \\ u(t) &= [0\ 1]\,\mathcal{H}(3)\boldsymbol{x}(3,t) \end{aligned} \tag{32}$$

with the initial state $\boldsymbol{x}(z,0) = \boldsymbol{0}$. According to (12), a flat output is given by

$$y(t) = [1\ 0]\,\mathcal{H}(0)\boldsymbol{x}(0,t) = \partial_t w(0,t). \tag{33}$$

New boundary conditions for (32) regarding (12),(14) are given by

$$\hat{\boldsymbol{x}}(0,t) = \mathcal{H}^{-1}(0) \begin{bmatrix} 0 & 1 \\ 1 & 0 \end{bmatrix} \begin{bmatrix} 0 \\ \hat{y}(s) \end{bmatrix} = \begin{bmatrix} 0 & \rho(0) \\ \frac{1}{\vartheta(0)} & 0 \end{bmatrix} \begin{bmatrix} 0 \\ y(t) \end{bmatrix}$$

so that

$$\hat{\boldsymbol{x}}(0,t) = \begin{bmatrix} \rho(0) \\ 0 \end{bmatrix} y(t) = \boldsymbol{m} y(t). \tag{34}$$

The matrices for (16a) in reference to (10) read $\Gamma_0(z) = 0$,

$$\Gamma_1(z) = \begin{bmatrix} 0 & \rho(z) \\ \frac{1}{\vartheta(z)} & 0 \end{bmatrix}, \quad \Gamma_0(z) = \begin{bmatrix} -\frac{\partial_z \rho(z)}{\rho(z)} & 0 \\ 0 & \frac{\partial_z \vartheta(z)}{\vartheta(z)} \end{bmatrix}.$$

Moreover, the input can be calculated directly as

$$u(t) = \vartheta(3) x_2(3,t). \tag{36}$$

The investigated problem is to achieve a steady state transition from the initial steady state $w_{0,\mathrm{s}}(z) = 0$ to the constant deflection $w_{\tau,\mathrm{s}}(z) = 1$. Note that all constant deflections $w(z,t)$ denote the steady state $\boldsymbol{x}_s(z) = \boldsymbol{0}$ according to (31). Subsequently, the investigated deflection trajectory to achieve this is given by the saturated and shifted ramp function

$$w_\zeta^*(0,t) = \begin{cases} 0, & t < \zeta, \\ \frac{t-\zeta}{\tau}, & t \in [\zeta, \zeta+\tau], \\ 1, & t > \zeta + \tau. \end{cases} \tag{37}$$

The transition time interval is given by $t \in [\zeta, \zeta+\tau]$ with $\tau = 1$ and $\zeta \geq 0$ is a variable to set a positive time shift. The corresponding flat output trajectory follows from (33) as $y(t) = \partial_t w^*(0,t)$. The feedforward input trajectory $u(t)$ can be calculated from (36) in terms of the parametrization by $y(t)$. The simulation results are subsequently obtained by using the finite element framework Firedrake (Rathgeber et al., 2016).

4.1 Constant parameters

If the parameters $\rho(z) = \rho$ and $\vartheta(z) = \vartheta$ are constant, then Remark 3 with $\Gamma(s) = \Gamma_1 s$ applies. The matrix

$$\Gamma_1 = \begin{bmatrix} 0 & \rho \\ \frac{1}{\vartheta} & 0 \end{bmatrix} \tag{38}$$

has two real eigenvalues $\gamma_{1,2} = \pm\sqrt{\rho/\vartheta}$, which are related to the inverse of the wave speed $c = \sqrt{\vartheta/\rho}$. Moreover, Γ_1 can be diagonalized using the matrix V, which is composed of the respective eigenvectors, i.e.,

$$V = \begin{bmatrix} -\sqrt{\rho\vartheta} & \sqrt{\rho\vartheta} \\ 1 & 1 \end{bmatrix}, \qquad V^{-1} = \frac{1}{2} \begin{bmatrix} -\frac{1}{\sqrt{\rho\vartheta}} & 1 \\ \frac{1}{\sqrt{\rho\vartheta}} & 1 \end{bmatrix}$$

to calculate the matrix exponential

$$e^{\Gamma(s)z} = e^{\Gamma_1 s z} = V \begin{bmatrix} e^{\gamma_1 s z} & 0 \\ 0 & e^{\gamma_2 s z} \end{bmatrix} V^{-1}. \tag{39}$$

Hence, the state parametrization evaluates to

$$\hat{\boldsymbol{x}}(z,s) = e^{\Gamma_1 s z}\boldsymbol{m}\hat{y}(s) = \frac{1}{2} \begin{bmatrix} \rho\left(e^{\frac{sz}{c}} + e^{-\frac{sz}{c}}\right) \\ \frac{1}{c}\left(e^{\frac{sz}{c}} - e^{-\frac{sz}{c}}\right) \end{bmatrix} \hat{y}(s), \tag{40}$$

which in the time domain corresponds to

$$\begin{aligned} x_1(z,t) &= \frac{\rho}{2}\left(y\left(t+\frac{z}{c}\right)\sigma\left(t+\frac{z}{c}\right) + y\left(t-\frac{z}{c}\right)\sigma\left(t-\frac{z}{c}\right)\right), \\ x_2(z,t) &= \frac{1}{2c}\left(y\left(t+\frac{z}{c}\right)\sigma\left(t+\frac{z}{c}\right) - y\left(t-\frac{z}{c}\right)\sigma\left(t-\frac{z}{c}\right)\right) \end{aligned}$$

with $\sigma(t)$ denoting the Heavyside step function. The input is given by (36) and reads

$$u(t) = \frac{y\left(t+\frac{3}{c}\right)\sigma\left(t+\frac{3}{c}\right) - y\left(t-\frac{3}{c}\right)\sigma\left(t-\frac{3}{c}\right)}{2c}. \tag{42}$$

As expected, the wave dynamics are reflected by time delayed and their advanced arguments of the flat output due to the finite speed of propagation. The input (42) generally allows a flat output $y(t)$ of any shape. However, there are two restrictions:

i) The flat output has to be piecewise continuous.
ii) The flat output has to be zero for $t < 3/c$, since $x_2(z,t)$ is only well-posed for $t \geq 0$ according to Sec. 2.

Consider the parameters $\rho = 4$, $\vartheta = 9$ and thus $c = 3/2$ and a target deflection $w_3^*(0,t)$. Fig. 1 shows the corresponding trajectories for the flat output and the input. The visualized input shows that the first non-zero

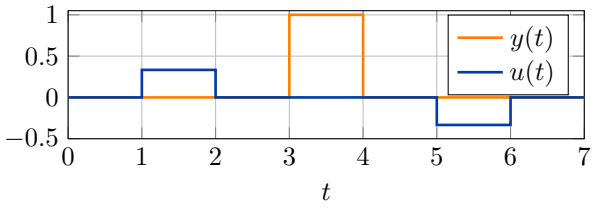

Fig. 1. Trajectories of the flat output and input (42) in the case of constant coefficients $\rho = 4$ and $\vartheta = 9$ ($c = 3/2$).

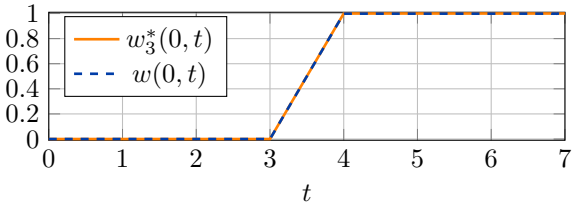

Fig. 2. Target wave deflection $w_3^*(0,t)$ and simulation result $w(0,t)$ in the case of constant coefficients $\rho = 4$ and $\vartheta = 9$ ($c = 3/2$).

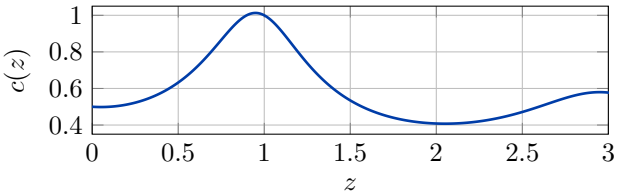

Fig. 3. Spatial variable wave speed $c(z) = \sqrt{\vartheta/\rho(z)}$ for parameters $\vartheta = 1$ and $\rho(z)$ as defined in (43).

contribution of (42) excites the system, while the second part compensates the backwards propagating reflection. Simulation results in terms of $w(0,t)$ are presented and compared with the target deflection in Fig. 2. Clearly, the simulation result matches the target one.

4.2 Spatially varying mass density

Consider a constant Young's modulus $\vartheta(z) = 1$ and a spatially varying mass density

$$\rho(z) = 2 + z + 2\cos(\pi z)\,. \tag{43}$$

The resulting spatial variable wave speed $c(z)$ is shown in Fig. 3. Using the formal integration approach according to Sec. 3.2, the Peano-Baker series (20)-(21) can practically only be evaluated for K matrix recursions and no closed form solution is available. Therefore, the numerical solution approach presented in Sec. 3.3, i.e., solving the Cauchy problem and using the inverse Laplace transformation is investigated in this case. The solution of the Cauchy problem is computed numerically using the LSODA algorithm. For numerical calculations, the target deflection (37) is shifted forward in time by a sufficiently large ζ to assure the time causality restriction in reference to ii) above. The used sampling points in terms of (28) are distributed linearly, i.e.,

$$t_k = t_0 + k\Delta t \tag{44}$$

with the constant step size Δt and $0 < t_0 < \zeta$. The input $u(t)$ is achieved by solving the port-Hamiltonian system (32) with the flat output as an input. Due to the large time

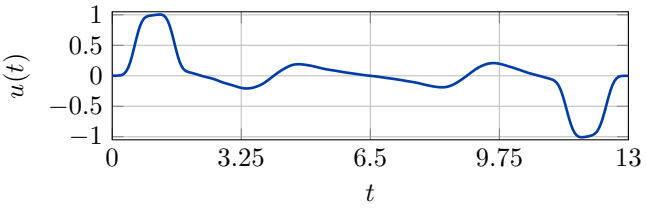

Fig. 4. Input trajectory determined by numerical inverse Laplace transformation for parameters $\vartheta = 1$ and $\rho(z)$ as defined in (43).

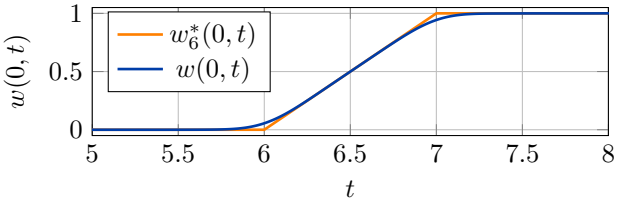

Fig. 5. Timeframe of the simulation output $w(0,t)$ for input $u(t)$ according to Fig. 4 and the shape of the related target wave deflection $w_6^*(0,t)$.

shift ζ, the result is then shifted backwards in time. Thus, the corresponding input starts at $t = 0$. The numerical result is shown in Fig. 4. The corresponding simulation output deflection $w(0,t)$ and the shape of the related target deflection $w_6^*(0,t)$ in terms of the input shifting are presented in Fig. 5. The overall slopes match each other except a small difference, especially at the edges of $w_6^*(0,t)$, where $w(0,t)$ shows a smooth characteristic. This results from the several stacked numerical approximations. As a result, the transition time interval in (37) is slightly widened, which has to be considered in the motion planning scheme. Summarized, the simulation result clearly shows the accomplishment of the target system behavior in terms of the steady state transition (37) by using the proposed numerical solution approach.

5. CONCLUSIONS

A constructive approach to motion planning for a class of boundary controlled port-Hamiltonian systems is introduced. The state and input are parametrized in terms of a so-called flat output by formulating Cauchy problem in the Laplace domain. The solution in the time domain is achieved by investigating two solution approaches. First, a formal integration approach is introduced. Secondly, a numerical approach is presented, where the Cauchy problem and the inverse Laplace transformation are computed numerically. The introduced approach is applied to the wave equation with constant and spatially varying parameters and validated by numerical simulation results. In the case of spatially varying parameters, the chosen numerical method shows a precise and efficient result. The application of the presented solutions to, e.g., port-Hamiltonian systems with internal energy dissipation or mixed boundary conditions, the closed loop control and optimal control for a constrained input are future research areas.

REFERENCES

Abate, J. and Whitt, W. (2006). A unified framework for numerically inverting Laplace transforms. *INFORMS Journal on Computing*, 18(4), 408–421.

Andrej, J. and Meurer, T. (2018). Flatness-based constrained optimal control of reaction-diffusion systems. In *American Control Conference (ACC)*, 2539–2544. Milwaukee (USA).

DaCunha, J.J. (2005). Transition matrix and generalized matrix exponential via the Peano-Baker series. *Journal of Difference Equations and Applications*, 11(15), 1245–1264.

Duindam, V., Macchelli, A., Stramigioli, S., and Bruyninckx, H. (2009). Port-Hamiltonian systems. In *Modeling and Control of Complex Physical Systems*, 53–130. Springer.

Dunbar, W., Petit, N., Rouchon, P., and Martin, P. (2003). Motion Planning for a nonlinear Stefan Problem. *European Series in Applied and Industrial Mathematics (ESAIM): Control, Optimization and Calculus of Variations*, 9.

Fliess, M., Levine, J., Martin, P., and Rouchon, P. (1999). A Lie-Backlund approach to equivalence and flatness of nonlinear systems. *IEEE Transactions on Automatic Control*, 44(5), 922–937.

Fliess, M., Lévine, J., Martin, P., and Rouchon, P. (1995). Flatness and defect of non-linear systems: introductory theory and examples. *International Journal of Control*, 61(6), 1327–1361.

Horváth, G., Horváth, I., Almousa, S.A.D., and Telek, M. (2020). Numerical inverse Laplace transformation using concentrated matrix exponential distributions. *Performance Evaluation*, 137, 102067.

Jacob, B. and Zwart, H.J. (2012). *Linear port-Hamiltonian systems on infinite-dimensional spaces*, volume 223. Springer Science & Business Media.

Laroche, B., Martin, P., and Rouchon, P. (2000). Motion planning for the heat equation. *International Journal of Robust and Nonlinear Control*, 10, 629–643.

Le Gorrec, Y., Zwart, H., and Maschke, B. (2005). Dirac structures and boundary control systems associated with skew-symmetric differential operators. *SIAM journal on Control and Optimization*, 44(5), 1864–1892.

Lynch, A. and Rudolph, J. (2002). Flatness-based boundary control of a class of quasilinear parabolic distributed parameter systems. *International Journal of Control*, 75.

Meurer, T. (2011). Flatness-based trajectory planning for diffusion-reaction systems in a parallelepipedon - a spectral approach. *Automatica*, 47, 935–949.

Meurer, T. (2012). *Control of Higher–Dimensional PDEs: Flatness and Backstepping Designs*. Springer Science & Business Media.

Meurer, T. and Kugi, A. (2009). Trajectory Planning for Boundary Controlled Parabolic PDEs With Varying Parameters on Higher-Dimensional Spatial Domains. *IEEE Transactions on Automatic Control*, 54, 1854 – 1868.

Meurer, T. and Zeitz, M. (2005). Feedforward and Feedback Tracking Control of Nonlinear Diffusion-Convection-Reaction Systems Using Summability Methods. *Industrial & Engineering Chemistry Research*, 44, 2532–2548.

Petit, N. and Rouchon, P. (2002). Dynamics and solutions to some control problems for water-tank systems. *IEEE Transactions on Automatic Control*, 47(4), 594–609.

Rathgeber, F., Ham, D.A., Mitchell, L., Lange, M., Luporini, F., McRae, A.T.T., Bercea, G.T., Markall, G.R., and Kelly, P.H.J. (2016). Firedrake: automating the finite element method by composing abstractions. *ACM Trans. Math. Softw.*, 43(3), 24:1–24:27. doi: 10.1145/2998441.

Rothfuß, R. (1997). *Anwendung der flachheitsbasierten Analyse und Regelung nichtlinearer Mehrgrößensysteme*. Fortschr.–Ber. VDI Reihe 8 Nr. 664. VDI Verlag, Düsseldorf.

Rothfuss, R., Rudolph, J., and Zeitz, M. (1996). Flatness based control of a nonlinear chemical reactor model. *Automatica*, 32(10), 1433 – 1439.

Rudolph, J. and Woittennek, F. (2008). Motion planning and open loop control design for linear distributed parameter systems with lumped controls. *International Journal of Control*, 81(3), 457–474.

Schörkhuber, B., Meurer, T., and Jüngel, A. (2013). Flatness of Semilinear Parabolic PDEs—A Generalized Cauchy–Kowalevski Approach. *IEEE Transactions on Automatic Control*, 58(9), 2277–2291.

van der Schaft, A. (2006). Port-Hamiltonian systems: an introductory survey. In *Proceedings of the International Congress of Mathematicians*, volume 3, 1339–1365.

Woittennek, F. (2011). On flatness and controllability of simple hyperbolic distributed parameter systems. *IFAC Proceedings Volumes*, 44(1), 14452–14457.

Appendix A. PEANO-BAKER SERIES

In the following, the limit of (19) in terms of (20),(21) is proven by mathematical induction.

Base case: For $k = 0$, we have

$$\hat{\boldsymbol{x}}^{[0]}(z,s) = M\hat{\boldsymbol{y}}(s) = \Lambda^{[0]}(z,t)M\hat{\boldsymbol{y}}(s)$$

and concluding $\Lambda^{[0]}(z,t) = I$.

Induktive step: Assuming that (20), (21) holds true for k, the case $k+1$ is investigated. Thus,

$$\begin{aligned}\hat{\boldsymbol{x}}^{[k+1]}(z,s) &= \hat{\boldsymbol{x}}^{[0]}(z,s) + \int_a^z \Gamma(\eta,s)\hat{\boldsymbol{x}}^{[k]}(\eta,s)\,\mathrm{d}\eta \\ &= M\hat{\boldsymbol{y}}(s) + \int_a^z \Gamma(\eta,s)\sum_{j=0}^{k}\Lambda^{[j]}(\eta,s)M\hat{\boldsymbol{y}}(s)\,\mathrm{d}\eta \\ &= \left(I + \int_a^z \Gamma(\eta,s)\sum_{j=0}^{k}\Lambda^{[j]}(\eta,s)\,\mathrm{d}\eta\right) M\hat{\boldsymbol{y}}(s).\end{aligned}$$

Interchanging the finite summation and integration yields

$$\int_a^z \Gamma(\eta,s)\sum_{j=0}^{k}\Lambda^{[j]}(\eta,s)\,\mathrm{d}\eta = \sum_{j=0}^{k}\int_a^z \Gamma(\eta,s)\Lambda^{[j]}(\eta,s)\,\mathrm{d}\eta.$$

Hence, the series can be reformulated as

$$\hat{\boldsymbol{x}}^{[k+1]}(z,s) = \left(I + \sum_{j=0}^{k}\int_a^z \Gamma(\eta,s)\Lambda^{[j]}(\eta,s)\,\mathrm{d}\eta\right) M\hat{\boldsymbol{y}}(s)$$

and the assertion follows.